HHS Public Access

Author manuscript

J Thorac Cardiovasc Surg. Author manuscript; available in PMC 2024 March 01.

Published in final edited form as:

J Thorac Cardiovasc Surg. 2023 March ; 165(3): e103–e116. doi:10.1016/j.jtcvs.2021.06.070.

Ex Vivo Biomechanical Analysis of the Ross Procedure Using the Modified Inclusion Technique in a 3D-Printed Left Heart Simulator

Yuanjia Zhu, MD[1,2], **Mateo Marin-Cuartas, MD**[1,3], **Matthew H. Park, MS**[1,4], **Annabel M. Imbrie-Moore, MS**[1,4], **Robert J. Wilkerson, BS**[1], **Sarah Madira, BS**[1], **Danielle M. Mullis, BS**[1], **Y. Joseph Woo, MD**[1,2]

[1]Department of Cardiothoracic Surgery, Stanford University, Stanford, CA

[2]Department of Bioengineering, Stanford University, Stanford, CA

[3]University Department of Cardiac Surgery, Leipzig Heart Center, Leipzig, Germany

[4]Department of Mechanical Engineering, Stanford University, Stanford, CA

Abstract

Objective—The inclusion technique was developed to reinforce the pulmonary autograft to prevent dilation after the Ross procedure. Anti-commissural plication (ACP), a modification technique, can reduce graft size and create neo-sinuses. The objective was to evaluate pulmonary valve biomechanics using the inclusion technique in the Ross procedure with and without ACP.

Methods—Seven porcine and five human pulmonary autografts were harvested from hearts obtained from a meat abattoir and from heart transplant recipients and donors, respectively. Five additional porcine autografts without reinforcement were used as controls. The Ross procedure was performed using the inclusion technique with a straight Dacron graft. The same specimens were tested both with and without ACP. Hemodynamic data, echocardiography, and high-speed videography were collected via the *ex vivo* heart simulator.

Results—Porcine autograft regurgitation was significantly lower after the use of inclusion technique compared to controls ($p<0.01$). ACP compared to non-ACP in both porcine and human pulmonary autografts was associated with lower leaflet rapid opening velocity (3.9±2.4 cm/s vs. 5.9±2.4 cm/s, $p=0.03$; 3.5±0.9 cm/s vs. 4.4±1.0 cm/s, $p=0.01$), rapid closing velocity (1.9±1.6 cm/s vs. 3.1±2.0 cm/s, $p=0.01$; 1.8±0.7 cm/s vs. 2.2±0.3 cm/s, $p=0.13$), relative rapid opening

Corresponding Author: Y. Joseph Woo, MD, 300 Pasteur Drive, Falk Cardiovascular Research Center, Department of Cardiothoracic Surgery, Stanford University School of Medicine, Stanford, CA 94305, P:650-725-3828; F:650-725-3846, joswoo@stanford.edu.

Disclosure

The authors have no conflicts of interest or financial relationships with industry to disclose.

DISCLOSURES

None.

force (4.6±3.0 vs. 7.7±5.2, p=0.03; 3.0±0.6 vs. 4.0±2.1, p=0.30), and relative rapid closing force (2.5±3.4 vs. 5.9±2.3, p=0.17; 1.4±1.3 vs. 2.3±0.6, p=0.25).

Conclusions—The Ross procedure using the inclusion technique demonstrated excellent hemodynamic results. The ACP technique was associated with more favorable leaflet biomechanics. *In vivo* validation should be performed to allow direct translation to clinical practice.

Keywords

Ross procedure; Pulmonary autograft; Aortic valve replacement; Pulmonary valve

INTRODUCTION

The Ross procedure is typically used to treat aortic valve dysfunction in children and young adults by replacing the aortic valve and aortic root with a pulmonary autograft and replacing the pulmonary valve with a pulmonary or aortic allograft.[1] This procedure enables the replacement of a diseased aortic valve with an autologous living substitute, which is advantageous because of its potential favorable hemodynamics, low endocarditis risk, low thrombogenicity, avoidance of anticoagulant therapy, and autograft growth which may be needed in children.[2] Although several studies demonstrated excellent outcomes associated with the Ross procedure[1–6], the need for reoperation remains the main limitation of the procedure.[7] One of the principal causes of failure of the pulmonary autograft is dilation of the neo-aortic root, subsequently leading to absence of central coaptation and regurgitation.[1,8,9] The inclusion technique using straight Dacron grafts was developed to reinforce the autograft by using a cylinder (Figure 1A–D, Video 1).[7] This technique was thought to prevent autograft late dilation, but information is sparse regarding the long-term outcomes.[9] Furthermore, anti-commissural plication (ACP), a modification technique, is commonly used in valve reimplantation procedures to recreate neo-sinuses that are geometrically similar to native aortic roots.[10] Though some evidence suggests that the vortices created by the sinuses are associated with stress reduction of the aortic leaflets[11–14], a recent study failed to demonstrate the added benefit of neo-sinuses in aortic leaflet hemodynamics and biomechanics in the valve-sparing root replacement procedure.[15] The objective of this study was to evaluate pulmonary valve biomechanics in the Ross procedure using the inclusion technique with and without ACP.

METHODS

Sample Preparation

Porcine pulmonary autografts (n = 7) were harvested from hearts obtained from a meat abattoir. To validate findings obtained from porcine specimens, human pulmonary autografts (n = 5) were obtained from heart transplant recipients and donors whose hearts were not used for transplantation (Figure 1E). During the harvest, care was taken to keep at least 2 mm of the right ventricular tissue below the nadir of each pulmonary leaflet attachment site (Figure 1F). Distally, the pulmonary artery 5 mm distal to the pulmonary valve commissures was discarded. Epicardial fat and any remaining adipose tissue on the pulmonary artery

were trimmed away to maximize the effective cross-sectional area of the neo-left ventricular outflow tract and the aortic root. Prepared pulmonary autografts were stored in vacuum sealed bags filled with normal saline in −20°C for no longer than 1 week until further use. When ready for ex vivo simulation, the pulmonary autografts were thawed in room temperature and then sized using an aortic valve sizer at the level of the commissures. Straight Dacron grafts that were 6–7 mm larger in diameter were selected. The average diameter of porcine pulmonary autografts was 20.0 ± 2.1 mm, and the Dacron grafts used averaged 26.8 ± 1.5 mm in diameter. The average diameter was 21.8 ± 1.8 mm for human pulmonary autografts with Dacron grafts sized 28.0 ± 2.4 mm in diameter used. The proximal suture line was first completed to attach the right ventricular tissue to the proximal end of the Dacron graft using a 4–0 polypropylene suture in a continuous fashion. Next, the three pulmonary valve commissures were suspended and fixed onto the Dacron graft using 4–0 polypropylene sutures (Figure 1G). The commissure suspension height and rotational degrees were adjusted to ensure proper coaptation of all three pulmonary valve leaflets. ACP was performed by plicating the Dacron graft between the commissures at the level of the commissures using a horizontal mattress stitch spanning roughly 2 mm on the Dacron graft above each cusp (Figure 1H, 1I). The final diameter of the Dacron graft after ACP was similar to the diameter of the pulmonary autograft at the level of the commissures. The distal end of the pulmonary autograft was then sutured onto the Dacron graft using a 4–0 polypropylene suture in a continuous fashion (Figure 1J). The proximal end of the finished reinforced pulmonary autograft was finally mounted to an elastomeric sewing ring on a 3D-printed conduit mount using a running 4–0 polypropylene suture (Figure 1K), and the distal Dacron graft was connected to a 3D-printed outflow mount. For the non-ACP group, there were no ACP sutures but the commissure attachment to the Dacron graft remained the same. From ACP to non-ACP or vice versa, the middle suture line connecting the distal pulmonary autograft and the Dacron graft was removed to allow the removal or addition of the ACP sutures, and the middle suture line was performed again after the ACP modification (Figure 1L). In this setup, the same specimens were used twice, one with ACP and the other without ACP in a random order. Additional photographs illustrating the steps to prepare the pulmonary autografts are shown in Figure S1.

To generate the control group, porcine pulmonary autografts without reinforcement were obtained from 5 additional hearts with the pulmonary autografts harvested in the same fashion as described above. The control right ventricular tissues were directly mounted to the conduit mount using a running 4–0 polypropylene suture. The distal pulmonary autograft and reinforced pulmonary autograft were connected to the outflow mount for *ex vivo* data collection.

Left Heart Simulator

The 3D-printed heart simulator (Figure 2A) was designed to allow for valvular investigations under physiologic conditions.[15–18] The simulator includes a programmable pulsatile linear piston pump (ViVitro Superpump, ViVitro Labs, Victoria, BC, Canada) that is attached to a custom left ventricular chamber to produce a physiologic waveform for in vitro valve testing in compliance with ISO 5840 standards. Ventricular, aortic, and left atrial pressure transducers (Utah Medical Products Inc., Midvale, Utah) as well as electromagnetic

flow probes (Carolina Medical Electronics, East Bend, North Carolina) were placed for hemodynamic measurement collection. Normal saline was used as the test fluid to ensure accurate transduction of the flow meters, and the temperature was set at 37°C. To calibrate the simulator, a mechanical disc valve (ViVitro) was placed in the mitral position while another mechanical disc valve was used in the aortic position. After calibration, the samples were placed in the aortic position, and hemodynamic data was collected and averaged for 10 cycles in each experimental phase, as per the standard recommendation from ViVitro Labs. High-speed videography from an *en face* perspective was also obtained at 1057 frames per second with 1280 × 1024 resolution (Chronos 1.4, Kron Technologies, Burnaby, British Columbia, Canada) to evaluate leaflet morphology and function.

Leaflet Motion Tracking

High-speed videography data were analyzed using Logger Pro®3 (Vernier) for leaflet motion tracking. Specifically, the noduli of all three cusps were tracked throughout a complete cardiac cycle (Figure 2B). Raw positional data were imported into MATLAB (R2020a, MathWorks Inc., Natick, MA) for data processing. A linear regression model was used to fit the displacement and velocity plots of each cusp during opening and closing to obtain velocity and acceleration, respectively. Results obtained from all three cusps during each phase were averaged to obtain the averaged cusp opening and closing velocity and relative force.

Echocardiography Measurements

Echocardiographic data were obtained using a Phillips iE33 system with an S5–1 transthoracic probe (Koninklijke Philips NV, Amsterdam, The Netherlands). Both short- and long-axis views were obtained from the side aortic root port with color flow mappings. Continuous-wave Doppler was obtained from the top aortic port. The iE33 on-board software and a Siemens Syngo Dynamics workstation (Siemens Medical Solutions USA, Inc., Ann Arbor, MI) was used for echocardiographic data analysis.

Statistical Analysis

To compare the ACP and non-ACP groups for both porcine and human specimens, repeated measures analysis of variance was performed with post-hoc correction. To compare the porcine control autograft without reinforcement to porcine specimens using the inclusion technique with or without ACP, a two-sampled t-test was performed after using F test to assess variance. Data analysis was performed in a blinded fashion. Continuous variables are reported as mean ± standard deviation unless otherwise specified. Statistical significance was defined at $p < 0.05$ for all tests. Based on our previous studies on aortic valve *ex vivo* simulations, to detect a 15% difference in mean regurgitant fraction with an estimated variance of 16, power of 80%, and confidence interval of 95%, a sample size of 2 is required. The use of human specimens received approval from the Institutional Review Board at Stanford University. Patient consent was provided for IRB #58850.

RESULTS

Valvular Hemodynamics

Figure 2C presents a representative example of the human pulmonary autograft without ACP captured by high-speed videography during diastole, whereas Figure 2D presents the same autograft with ACP. Example high-speed videography footages obtained from a porcine autograft are shown in Video S1 and S2. Note that although proper coaptation was reproduced with and without ACP, the pulmonary valve appeared to have improved coaptation height and increased excess tissue when ACP was used with changes in cusp fluttering pattern during systole via qualitative assessment. Compared to porcine control pulmonary autograft without reinforcement (Video S3), the inclusion technique with or without ACP demonstrated larger cusp coaptation height with higher cusp fluttering speed during systole. The control autograft without reinforcement distended under the systemic pressure, leading to visible central leakage.

Mean aortic flow tracings and pressure tracings of the porcine and human specimens are shown in Figure 3, with shaded regions representing standard deviation. No significant regurgitation was observed from the mean aortic flow tracings in either porcine or human specimens with or without ACP. However, porcine control autograft without reinforcement demonstrated higher regurgitant fractions (17.0 ±5.6%) compared to porcine pulmonary autografts with ACP (7.5 ± 3.1%, $p = 0.01$) and without APC (5.5 ± 2.5%, $p = 0.001$). Pulmonary autograft regurgitant fractions using human autografts were 9.0 ± 2.5% and 10.7 ± 5.3% ($p = 0.58$), respectively. A summary of hemodynamics data is shown in Table 1 and Table S1. Additionally, transvalvular hemodynamics were similar with and without ACP for both porcine and human specimens, as evidenced by 2D echocardiography. For porcine pulmonary autografts with and without ACP, the mean gradients were 14.3 ± 10.2 mmHg vs. 11.1 ± 4.4 mmHg ($p = 0.37$), respectively. Compared to the mean gradient measured from porcine control pulmonary autografts without reinforcement (4.2 ± 1.2 mmHg), the mean gradient of porcine pulmonary autografts without ACP were significantly higher ($p = 0.01$), but ACP was associated with similar mean gradient ($p = 0.06$). For human pulmonary autografts with and without ACP, the mean gradients were 12.8 ± 5.1 mmHg vs. 13.8 ± 5.2 mmHg ($p = 0.49$), respectively.

Valvular Kinematics

Leaflet motion tracking analysis of high-speed videometric data demonstrated that ACP compared to non-ACP in porcine pulmonary autografts was associated with lower leaflet rapid opening velocity (3.9 ± 2.4 cm/s vs. 5.9 ± 2.4 cm/s, $p = 0.03$), leaflet rapid closing velocity (1.9 ± 1.6 cm/s vs. 3.1 ± 2.0 cm/s, $p = 0.01$), relative leaflet rapid opening force (4.6 ± 3.0 vs. 7.7 ± 5.2, $p = 0.03$), and relative leaflet rapid closing force (2.5 ± 3.4 vs. 5.9 ± 2.3, $p = 0.17$) (Figure 4). In comparison, porcine control pulmonary autografts without reinforcement showed leaflet rapid opening velocity of 3.6 ± 0.3 cm/s, which was significantly lower than that from porcine autografts without ACP ($p = 0.05$) but similar to that from porcine autografts with ACP ($p = 0.77$). Leaflet rapid closing velocity (2.3 ± 0.4 cm/s), relative leaflet rapid opening force (3.2 ± 0.2), and relative leaflet rapid closing force (3.0 ± 0.5) of porcine control pulmonary autografts without reinforcement were similar to

those of porcine autografts using the inclusion technique with or without ACP ($p > 0.06$). Similar findings were observed in the human pulmonary autografts with vs. without ACP in terms of leaflet rapid opening velocity (3.5 ± 0.9 cm/s vs. 4.4 ± 1.0 cm/s, $p = 0.01$), leaflet rapid closing velocity (1.8 ± 0.7 cm/s vs. 2.2 ± 0.3 cm/s, $p = 0.14$), relative leaflet rapid opening force (3.0 ± 0.6 vs. 4.0 ± 2.1, $p = 0.30$), and relative leaflet rapid closing force (1.4 ± 1.3 vs. 2.3 ± 0.6, $p = 0.25$) (Figure 4).

DISCUSSION

In this study, we successfully recreated a highly clinically relevant *ex vivo* Ross procedure model (Figure 5). The ability to study the Ross procedure in a precisely controlled *ex vivo* environment is greatly beneficial to the understanding of the Ross procedure and its potential benefits and complications. The utility of the Ross procedure remains controversial, primarily due to the graft failure rate observed during the second decade of follow up.[19] With the development of this *ex vivo* model, we can systematically evaluate different variations of the Ross procedure and elucidate the biomechanics and valvular functions associated with each technique.

We demonstrated that the Ross procedure using the inclusion technique was associated with excellent hemodynamic results using both porcine and human autografts. In fact, the use of inclusion technique was associated with significantly improved pulmonary autograft regurgitant fraction compared to control autografts without reinforcement. As pulmonary valves do not have anatomical annulus, the neo-aortic roots therefore are easily distensible. Through the high-speed videography, we consistently observed low cusp coaptation height, which is likely one of the main causes of a higher regurgitant fraction observed in the control specimens. The Dacron grafts used in the inclusion technique provide structural and mechanical support to the neo-aortic roots. Although it was associated with a small increase in mean transvalvular gradient, the difference may not be clinically significant. Additionally, the use of ACP not only preserved the advantage of improved cusp coaptation, but it also demonstrated similar mean transvalvular gradient compared to that from the control specimens. Furthermore, the application of ACP was associated with significantly decreased leaflet rapid opening and closing velocities and relative leaflet rapid opening force. It was also associated with a decreased trend in relative leaflet rapid closing force in the porcine autografts. All the above parameters measured from the autografts with ACP were similar to those obtained from the control specimens. An increase in rapid leaflet movement velocity and forces can potentially have a negative impact on the long-term durability of the autograft tissue, leading to repair failure. In fact, degeneration of the neo-aortic valve was found to be a common pathologic outcome of the Ross procedure, regardless of the technique used for its transfer into the aortic position.[3,9,20,21] Interestingly, although it has been hypothesized that the ACP technique by creating neo-sinuses may provide added valvular hemodynamic benefits[11–14], its long-term impact compared to using straight graft alone for valve reimplantation remains unclear. Our prior *ex vivo* study also did not demonstrate biomechanical advantages of neo-sinuses.[15] In this study, ACP was associated with more favorable leaflet kinematics compared to without ACP. This may be due to the appropriate graft sizing and the inherent tissue property differences between the pulmonic and aortic

root. The use of ACP therefore, may potentially prevent the autograft valve from early failure by improving leaflet biomechanics.

In the human specimens, we similarly observed that ACP was associated with significantly decreased leaflet opening velocity in addition to a trend towards decreased leaflet closing velocity and decreased opening and closing relative forces. Though porcine hearts have been frequently selected as a human analog due to similarities in size and anatomy to human valves[22,23], differences exist in tissue mechanical properties and cusp thickness between human and porcine pulmonary valves.[24,25] These discrepancies may have ultimately resulted in the differences in valvular biomechanics between porcine and human specimens observed in this study. One of the common critiques of modeling studies using animal specimens is their poor translatability to clinical application due to the intrinsic differences, even though they can be minor, between the animal specimens and human samples. In this study, we showed comparable findings in the biomechanics advantage of using ACP in Ross procedure with the inclusion technique. The results obtained from the human autografts provided additional validity to the findings in this study.

The use of ACP in the Ross procedure with the inclusion technique was driven by the discrepancy in the diameters of right ventricular outflow tract and the pulmonary artery in humans.[26,27] Interestingly, we observed similar findings in the porcine specimens where the diameter of the pulmonary autograft quickly tapers down from the right ventricular outflow tract to the pulmonary artery at the level of the commissures. Due to this anatomic finding, the selection of properly sized straight aortic grafts becomes more difficult. Undersizing the Dacron graft to accommodate for the diameter of the pulmonary artery would lead to obstruction in the neo-aortic root, causing aortic stenosis. However, selecting a Dacron graft that fits the right ventricular outflow tract in the fully distended state under the system pressure would inevitably result in the distortion of the commissures radially outwards. This geometric distortion can falsely enlarge the neo-aortic root diameter, which may contribute to improper leaflet coaptation and subsequently valvular regurgitation, likely similar to the central leakage that was observed in the porcine control autografts without reinforcement. We elected to use a straight Dacron graft that is 6–7 mm larger in diameter than that of the pulmonary autograft to account for the diameter and thickness of the right ventricular wall tissue at the level of the nadirs of pulmonary cusps. As much of the adipose and excess tissue as possible should be trimmed away to further minimize narrowing of the neo-aortic roots. The use of ACP can further minimize the size discrepancy between the proximal and distal end of the pulmonary autografts by reducing the Dacron graft diameter at the level of the commissures. Interestingly, with this Dacron graft sizing, excess cusp tissue with slightly eccentric central coaptation zone was still observed compared to those from porcine control autografts without reinforcement. Differences in pulmonary cusp thickness and mechanical properties of pulmonary valves, roots, and right ventricular outflow tracts compared to those of aortic valves and roots may all contribute to the different valve behaviors observed using pulmonary versus aortic valves for reimplantation.[15,28] Although clinically significant autograft stenosis was not observed, it would be prudent to analyze the impact of different reinforcement graft size on pulmonary valvular hemodynamics and leaflet motion in the future.

A few limitations exist in this study. One limitation is the inability to fully simulate *in vivo* cardiac motion and the associated complex helical flow patterns generated by the left ventricle.[29,30] Although our simulator generates physiologic waveforms, the left ventricular chamber and the aortic outflow conduit differ from the physiologic geometry and material properties of the native tissue and can lead to elevated peak transvalvular velocity. Ventricular contractions and variable flow profiles across the neo-aortic valve may have an effect on valve hemodynamics. *In vivo* pre-clinical large animal studies may be indicated to address this limitation and to allow detailed analysis of flow profiles across the pulmonary autograft. Additionally, even though we validated our findings obtained from porcine specimens by using human samples, these human specimens were either obtained from patients with end-stage cardiomyopathy selected for heart transplantation or from donor hearts not suitable for transplantation. Differences exist in abnormal tissues compared to those obtained from healthy patients or patients with aortic valve diseases. However, this issue may unfortunately be the nature of human tissue-based research and may not be ethically addressed. Another interesting aspect that may warrant further investigation is the impact of pulmonary valve orientation in the neo-aortic root, given the slight difference in cusp size and flow dynamics in the native pulmonary artery system. Lastly, this *ex vivo* study focused on the short-term outcomes after using two different repair techniques. Long-term outcomes are needed to further guide clinical practice. Nonetheless, our study allowed for a controlled and reproducible evaluation of different surgical repair options on the same specimen, which would be impossible in clinical practice. This study also elucidated the differences in valve biomechanics in the Ross procedure using the inclusion technique with and without ACP. These findings will not only guide future studies to further investigate the biomechanics behind the Ross procedure but may also direct future innovations to improve clinical outcomes.

In conclusion, the Ross procedure using the inclusion technique demonstrated excellent hemodynamic results. The ACP technique was associated with more favorable leaflet biomechanics, potentially improving the long-term durability of the pulmonary autografts. *In vivo* validation should be performed to allow for direct translation to clinical practice.

Supplementary Material

Refer to Web version on PubMed Central for supplementary material.

ACKNOWLEDGMENTS

This work was supported by the National Institutes of Health (NIH R01 HL152155 and NIH R01 HL089315-01, YJW), the Thoracic Surgery Foundation Resident Research Fellowship (YZ), the National Science Foundation Graduate Research Fellowship Program (DGE-1656518, AMI), and a Stanford Graduate Fellowship (AMI). We would also like to thank the generous donation by Mr. M. Ian Ritchie to support this research effort.

Funding

This work was supported by the National Institutes of Health (NIH R01 HL152155 and NIH R01 HL089315-01, YJW), the Thoracic Surgery Foundation Resident Research Fellowship (YZ), the National Science Foundation Graduate Research Fellowship Program (AMI), and a Stanford Graduate Fellowship (DGE-1656518, AMI). The content is solely the responsibility of the authors and does not necessarily represent the official views of the funders.

Patient consent was provided for IRB #58850.

Biography

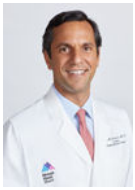

Glossary of Abbreviations

ACP	anti-commissural plication
RMS	root mean square
SD	standard deviation

REFERENCES

1. Kouchoukos NT, Masetti P, Nickerson NJ, Castner CF, Shannon WD, Dávila-Román VG. The Ross procedure: Long-term clinical and echocardiographic follow-up. Ann Thorac Surg 2004;78:773–81. [PubMed: 15336990]
2. Takkenberg JJ, Klieverik LM, Schoof PH, van Suylen RJ, van Herwerden LA, Zondervan PE, et al. The Ross procedure: A systematic review and meta-analysis. Circulation 2009;119:222–8. [PubMed: 19118260]
3. David TE, David C, Woo A, Manlhiot C. The Ross procedure: outcomes at 20 years. J Thorac Cardiovasc Surg 2014;147:85–93. [PubMed: 24084276]
4. Brown JW, Ruzmetov M, Shahriari A, Rodefeld MD, Turrentine MW, Mahomed Y. The Ross full root replacement in adults with bicuspid aortic valve disease. J Heart Valve Dis 2011;20:332–9. [PubMed: 21714426]

5. Charitos EI, Takkenberg JJ, Hanke T, Gorski A, Botha C, Franke U, et al. Reoperations on the pulmonary autograft and pulmonary homograft after the Ross procedure: An update on the German Dutch Ross Registry. J Thorac Cardiovasc Surg 2012;144:813–21. [PubMed: 22883549]
6. Mazine A, Rocha RV, El-Hamamsy I, Ouzounian M, Yanagawa B, Bhatt DL, et al. Ross Procedure vs Mechanical Aortic Valve Replacement in Adults: A Systematic Review and Meta-analysis. JAMA Cardiol 2018;3:978–87. [PubMed: 30326489]
7. Elkins RC, Lane MM, McCue C. Pulmonary autograft reoperation: incidence and management. Ann Thorac Surg 1996;62:450–5. [PubMed: 8694604]
8. de Kerchove L, Rubay J, Pasquet A, Poncelet A, Ovaert C, Pirotte M, et al. Ross operation in the adult: long-term outcomes after root replacement and inclusion techniques. Ann Thorac Surg 2009;87:95–102. [PubMed: 19101277]
9. David TE, Omran A, Ivanov J, Armstrong S, de Sa MP, Sonnenberg B, et al. Dilation of the pulmonary autograft after the Ross procedure. J Thorac Cardiovasc Surg 2000;119:210–20. [PubMed: 10649195]
10. Gleason TG. New graft formulation and modification of the David reimplantation technique. J Thorac Cardiovasc Surg 2005;130:601–3. [PubMed: 16077451]
11. De Paulis R, De Matteis GM, Nardi P, Scaffa R, Buratta MM, Chiariello L. Opening and closing characteristics of the aortic valve after valve-sparing procedures using a new aortic root conduit. Ann Thorac Surg 2001;72:487–94. [PubMed: 11515887]
12. Leyh RG, Schmidtke C, Sievers HH, Yacoub MH. Opening and closing characteristics of the aortic valve after different types of valve-preserving surgery. Circulation 1999;100:2153–60. [PubMed: 10571974]
13. Schmidtke C, Sievers HH, Frydrychowicz A, Petersen M, Scharfschwerdt M, Karluss A, et al. First clinical results with the new sinus prosthesis used for valve-sparing aortic root replacement. Eur J Cardiothorac Surg 2013;43:585–90. [PubMed: 22665384]
14. Charitos EI, Sievers HH. Anatomy of the aortic root: implications for valve-sparing surgery. Ann Cardiothorac Surg 2013;2:53–6. [PubMed: 23977559]
15. Paulsen MJ, Imbrie-Moore AM, Baiocchi M, Wang H, Hironaka CE, Lucian HJ, et al. Comprehensive Ex Vivo Comparison of 5 Clinically Used Conduit Configurations for Valve-Sparing Aortic Root Replacement Using a 3-Dimensional-Printed Heart Simulator. Circulation 2020;142:1361–73. [PubMed: 33017215]
16. Zhu Y, Imbrie-Moore AM, Park MH, Paulsen MJ, Wang H, MacArthur JW, et al. Ex Vivo Analysis of a Porcine Bicuspid Aortic Valve and Aneurysm Disease Model. Ann Thorac Surg 2020:S0003-4975(20)31122-X.
17. Zhu Y, Imbrie-Moore AM, Paulsen MJ, Priromprintr B, Wang H, Lucian HJ, et al. Novel bicuspid aortic valve model with aortic regurgitation for hemodynamic status analysis using an ex vivo simulator. J Thorac Cardiovasc Surg 2020:S0022-5223(20)31749-9.
18. Zhu Y, Imbrie-Moore AM, Paulsen MJ, Priromprintr B, Park MH, Wang H, et al. A Novel Aortic Regurgitation Model from Cusp Prolapse with Hemodynamic Validation Using an Ex Vivo Left Heart Simulator. J Cardiovasc Transl Res 2020. doi: 10.1007/s12265-020-10038-z.
19. Mokhles MM, Rizopoulos D, Andrinopoulou ER, Bekkers JA, Roos-Hesselink JW, Lesaffre E, et al. Autograft and pulmonary allograft performance in the second post-operative decade after the Ross procedure: insights from the Rotterdam Prospective Cohort Study. Eur Heart J 2012;33(17):2213–24. [PubMed: 22730489]
20. Elkins RC, Thompson DM, Lane MM, Elkins CC, Peyton MD. Ross operation: 16-year experience. J Thorac Cardiovasc Surg 2008;136:623–30. [PubMed: 18805263]
21. David TE, Woo A, Armstrong S, Maganti M. When is the Ross operation a good option to treat aortic valve disease? J Thorac Cardiovasc Surg 2010;139:68–73. [PubMed: 20106360]
22. Benhassen LL, Ropcke DM, Sharghbin M, Lading T, Skov JK, Tjørnild MJ, et al. Comparison of Dacron ring and suture annuloplasty for aortic valve repair-a porcine study. Ann Cardiothorac Surg 2019;8:342–50. [PubMed: 31240178]
23. Wang C, Lachat M, Regar E, von Segesser LK, Maisano F, Ferrari E. Suitability of the porcine aortic model for transcatheter aortic root repair. Interact Cardiovasc Thorac Surg. 2018;26:1002–8. [PubMed: 29415164]

24. Stradins P, Lacis R, Ozolanta I, Purina B, Ose V, Feldmane L, et al. Comparison of biomechanical and structural properties between human aortic and pulmonary valve. Eur J Cardiothorac Surg 2004;26:634–9. [PubMed: 15302062]

25. Christie GW, Barratt-Boyes BG. Mechanical properties of porcine pulmonary valve leaflets: How do they differ from aortic leaflets? Ann Thorac Surg 1995;60:195–9.

26. Truong QA, Massaro JM, Rogers IS, Mahabadi AA, Kriegel MF, Fox CS, et al. Reference values for normal pulmonary artery dimensions by noncontrast cardiac computed tomography: the Framingham Heart Study. Circ Cardiovasc Imaging 2012;5:147–54. [PubMed: 22178898]

27. Izumo M, Shiota M, Saitoh T, Kuwahara E, Fukuoka Y, Gurudevan SV, et al. Non-circular shape of right ventricular outflow tract: a real-time 3-dimensional transesophageal echocardiography study. Circ Cardiovasc Imaging 2012;5:621–7. [PubMed: 22891043]

28. Paulsen MJ, Kasinpila P, Imbrie-Moore AM, Wang H, Hironaka CE, Koyano TK, et al. Modeling conduit choice for valve-sparing aortic root replacement on biomechanics with a 3-dimensional-printed heart simulator. J Thorac Cardiovasc Surg 2019;158:392–403. [PubMed: 30745047]

29. Stoll VM, Hess AT, Rodgers CT, Bissell MM, Dyverfeldt P, Ebbers T, et al. Left Ventricular Flow Analysis. Circ Cardiovasc Imaging 2019;12(5):e008130. [PubMed: 31109184]

30. Faludi R, Szulik M, D'hooge J, Herijgers P, Rademakers F, Pedrizzetti G, et al. Left ventricular flow patterns in healthy subjects and patients with prosthetic mitral valves: an in vivo study using echocardiographic particle image velocimetry. J Thorac Cardiovasc Surg 2010;139:1501–10. [PubMed: 20363003]

CENTRAL PICTURE

Intraoperative (A), human (B), and porcine (C) pulmonary autograft for the Ross procedure.

CENTRAL MESSAGE

Anti-commissural plication was associated with favorable leaflet biomechanics in the Ross procedure with the inclusion technique.

PERSPECTIVE STATEMENT

The need for reoperation remains the main limitation of the Ross procedure. We showed that the Ross procedure using the inclusion technique was associated with excellent hemodynamics. Anti-commissural plication was associated with improved leaflet biomechanics. These findings will help direct surgical techniques and innovations to improve clinical outcomes after the Ross procedure.

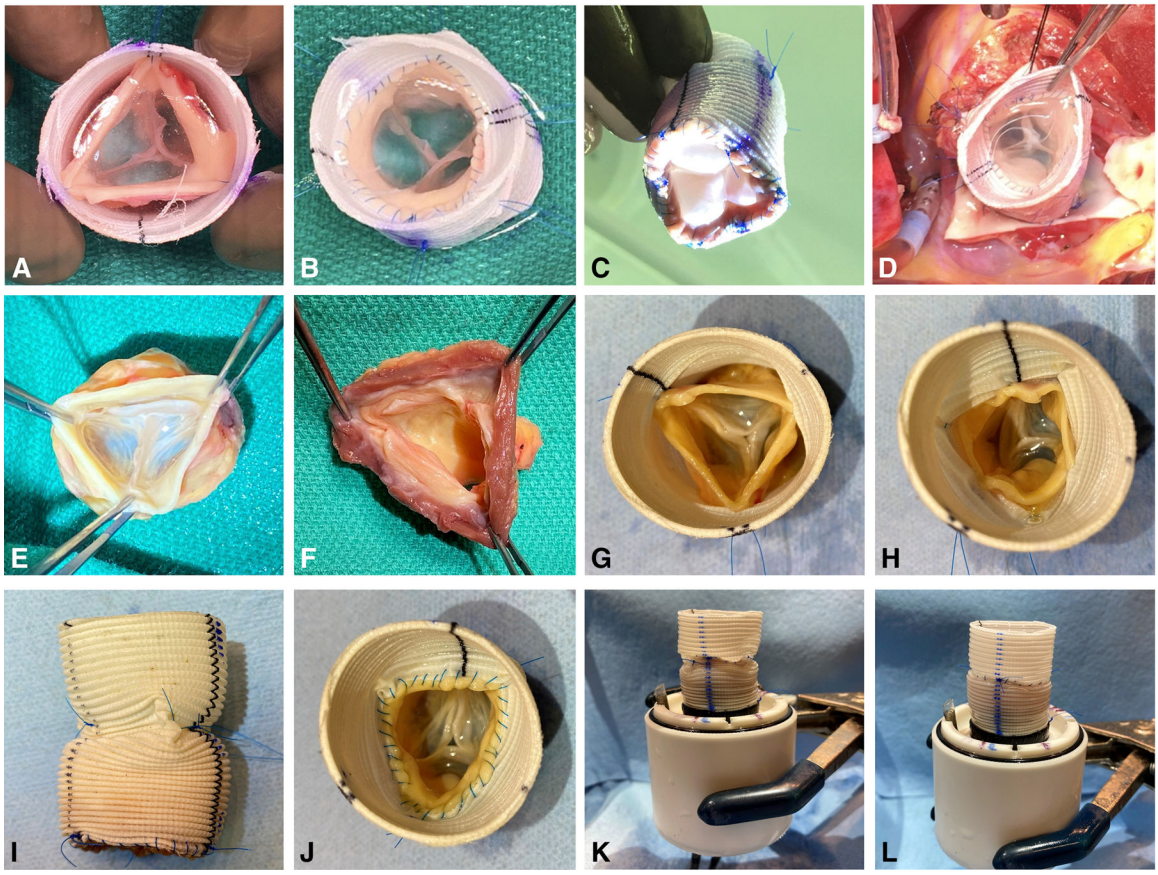

Figure 1:

An intraoperative photographic example of the use of the inclusion technique in a Ross procedure (A-D) and detailed surgical steps for pulmonary autograft preparation using the inclusion technique with anti-commissural plication (E-J) for ex vivo simulation experiments (K, L). (A) An intraoperative photograph of a pulmonary autograft harvested and being prepared using the inclusion technique for the Ross procedure. The three commissures were suspended and attached to a straight Dacron graft. Note the proper leaflet coaptation. (B) The distal pulmonary autograft attached to the Dacron graft. Note the competent pulmonary valve. (C) The neo-ventricular view of the same pulmonary autograft. (D) The same pulmonary autograft implanted in the left ventricular outflow tract as the neo-aortic root with excellent valve competency. (E) Human pulmonary autograft harvested. Note the competent pulmonary cusps with proper coaptation. (F) At least 2 mm of the right ventricular tissue proximal to the nadir of each pulmonary leaflet attachment site was saved. (G) Pulmonary valve commissures suspended and fixed onto the straight Dacron graft. (H) Anti-commissural plication performed to plicate the graft between the commissures at the level of the commissures. (I) The side view of the Dacron graft after anti-commissural plication. (J) The middle suture line attaching the distal pulmonary autograft and the Dacron graft. (K) The composite pulmonary autograft with anti-commissural plications mounted onto an elastomeric sewing ring on a 3D-printed conduit mount for *ex vivo* testing. (L) The same composite pulmonary autograft without anti-commissural plication sutures.

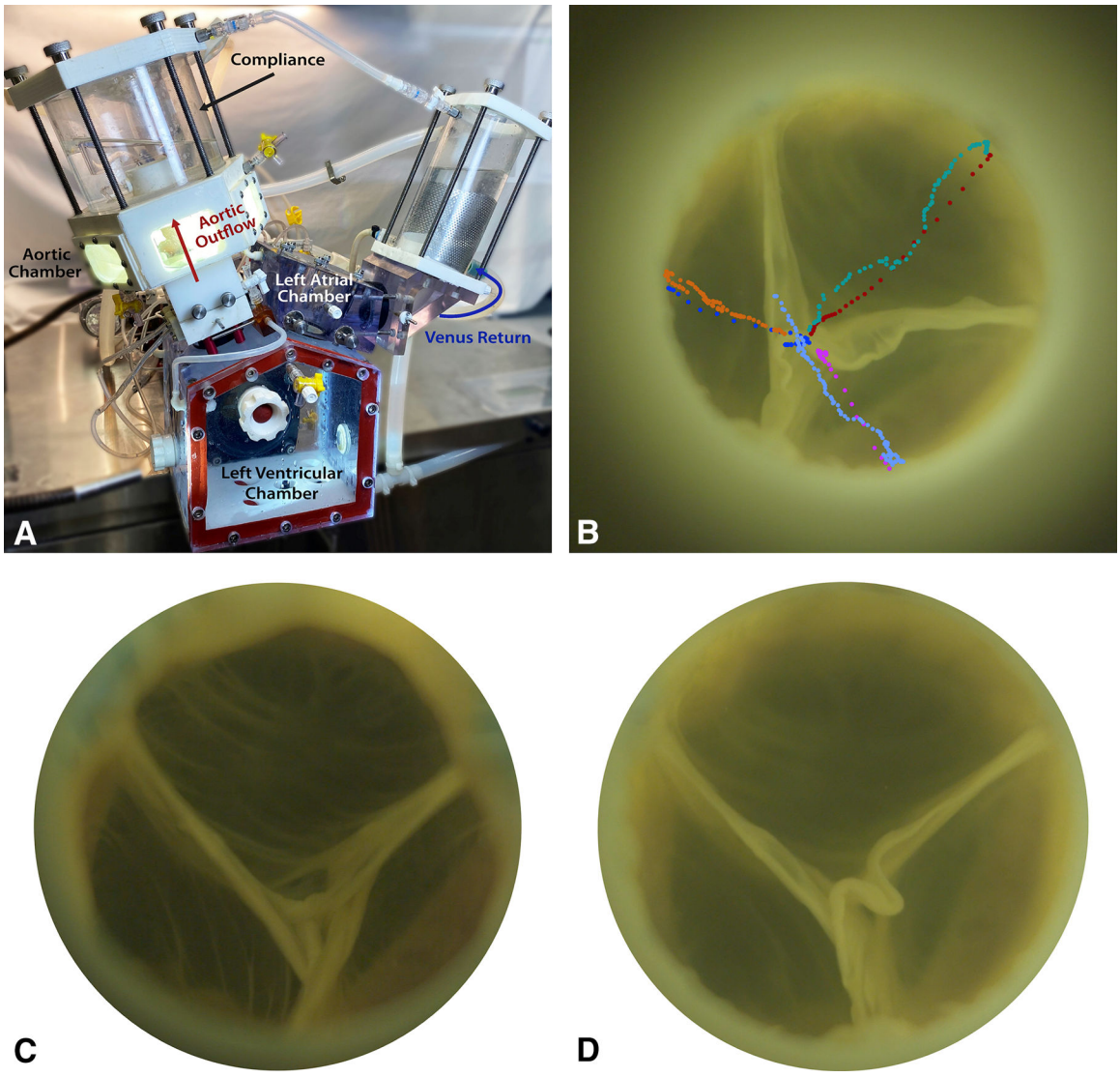

Figure 2:

(A) Diagram of the ex vivo left heart simulator. (B) An example of leaflet motion tracking analysis. Each marker represents the position of the nodulus of each leaflet at each time frame captured by high-speed videography. Each color represents each leaflet during either opening or closing. (C) An *en face* view of a human pulmonary valve without using anti-commissural plications captured by high-speed videography during diastole. (D) The same human pulmonary valve with anti-commissural plications captured by high-speed videography during diastole. The pulmonary valve appeared to have slightly improved coaptation height when anti-commissural plication was used.

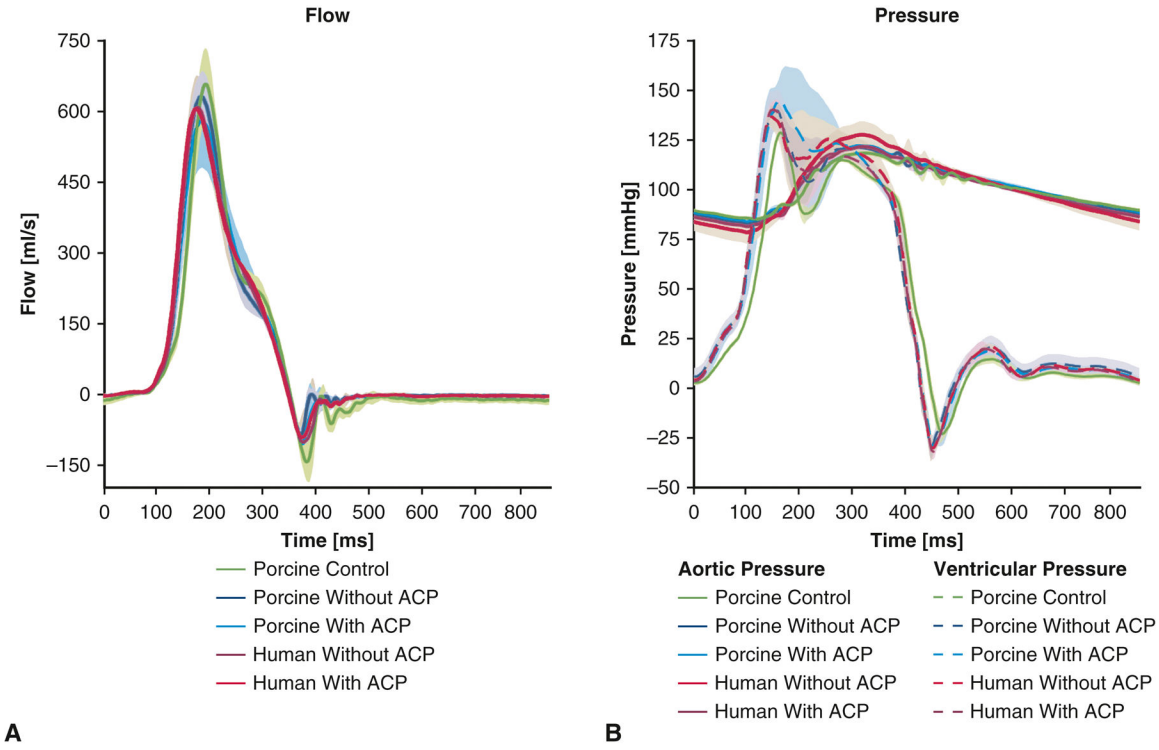

Figure 3:

(A) Aortic flow measurements of porcine control pulmonary autografts without reinforcement, as well as porcine and human pulmonary autografts using the inclusion technique with and without anti-commissural plications. The aortic flow profiles were overall similar among the five groups. Porcine control pulmonary autografts without reinforcement demonstrated increased flow reversal during diastole, suggesting increased valve regurgitation. (B) Pressure measurements of porcine control pulmonary autografts without reinforcement, as well as porcine and human pulmonary autografts using the inclusion technique with and without anti-commissural plications. The pressure tracings were overall similar among the five groups. Shaded regions represent standard deviation. ACP = anti-commissural plication.

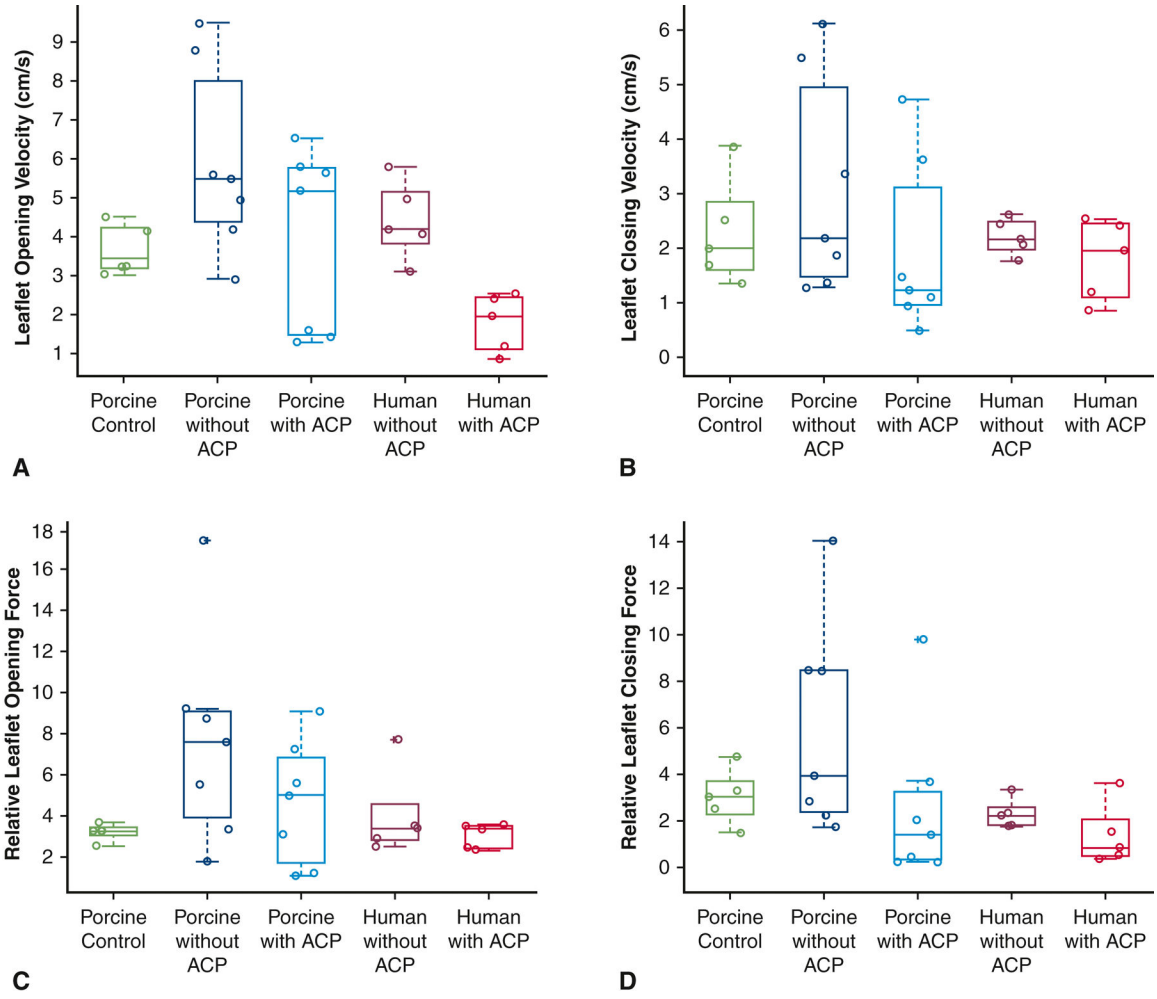

Figure 4:

Leaflet motion tracking analysis performed to elucidate leaflet opening velocity (A), leaflet closing velocity (B), relative leaflet opening force (C) and relative leaflet closing force (D) of porcine control pulmonary autografts without reinforcement, and porcine and human specimens using the inclusion technique with and without anti-commissural plication. ACP compared to non-ACP in porcine pulmonary autografts was associated with lower leaflet rapid opening velocity ($p = 0.03$), leaflet rapid closing velocity ($p = 0.01$), relative leaflet rapid opening force ($p = 0.03$), and relative leaflet rapid closing force ($p = 0.17$). In comparison, porcine control pulmonary autografts without reinforcement showed lower leaflet rapid opening velocity than that from porcine autografts without ACP ($p = 0.05$) but was similar to that from porcine autografts with ACP ($p = 0.77$). Porcine control pulmonary autografts without reinforcement had similar leaflet rapid closing velocity, relative leaflet rapid opening force, and relative leaflet rapid closing force compared to those from porcine autografts using the inclusion technique with or without ACP. In human autografts, ACP was associated with lower leaflet rapid opening velocity than without ACP ($p = 0.01$). The upper and lower borders of each box represent the upper and lower quartiles. The middle horizontal line represents the median. Each data point was plotted with circles. The extra + represents outlier. ACP = anti-commissural plication.

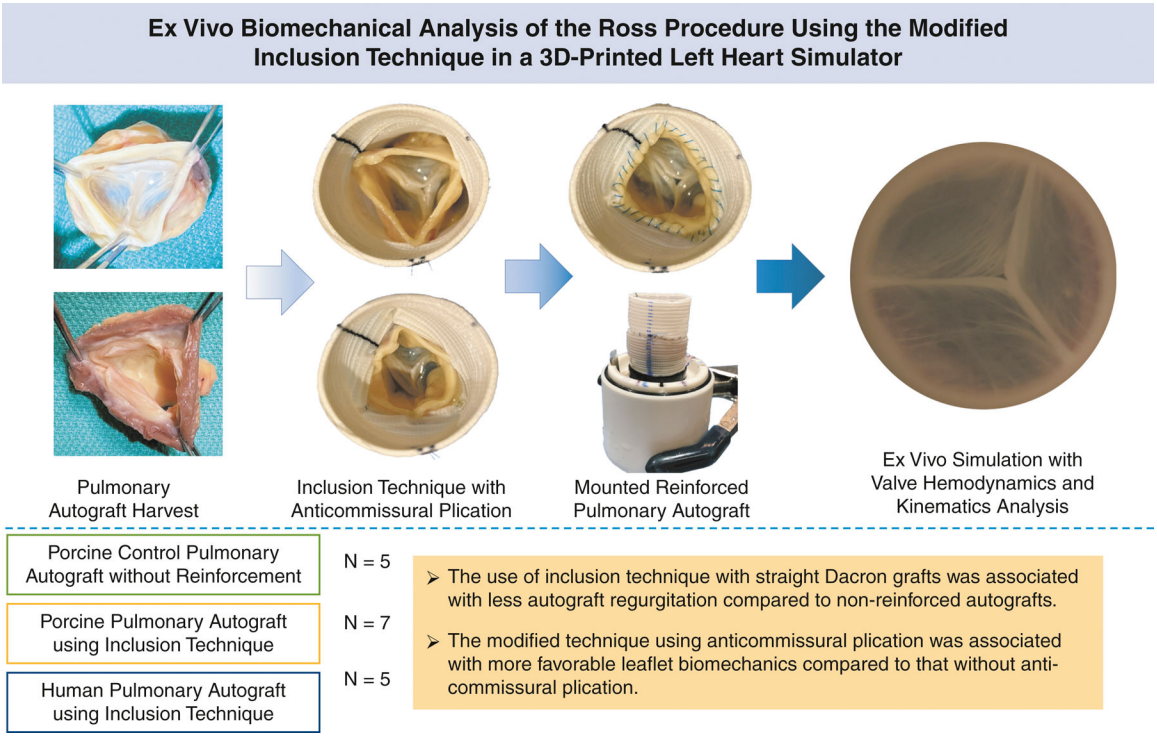

Figure 5:

Ross procedure using the inclusion technique with straight Dacron grafts with or without anti-commissural plication was evaluated using an *ex vivo* left heart simulator for valvular hemodynamics and kinematics analysis.

Video 1:

A video illustrating the operative steps of the Ross procedure using the inclusion technique via a straight Dacron graft with anti-commissural plication.

Table 1:

Hemodynamic characteristics of porcine and human pulmonary autografts using the inclusion technique with and without anti-commissural plications.

	Porcine Autograft with ACP N = 7 Mean±SD	Porcine Autograft without ACP N = 7 Mean±SD	Porcine Autograft ACP vs. non-ACP *P* value	Human Autograft with ACP N = 5 Mean±SD	Human Autograft without ACP N = 5 Mean±SD	Human Autograft ACP vs. non-ACP *P* value
Heart rate (bpm)	70.0±0.0	70.0±0.0	1.00	70.0±0.0	70.0±0.0	1.00
Mean arterial pressure (mmHg)	98.0±7.3	97.0±6.9	0.06	100.0±0.5	100.8±1.0	0.14
Systolic pressure (mmHg)	113.7±16.8	112.4±16.6	0.03*	121.7±0.6	127.8±6.5	0.12
Diastolic pressure (mmHg)	84.5±1.6	83.2±1.8	<.001*	81.4±0.7	78.2±5.6	0.30
Cardiac output (liters/min)	4.7±0.2	4.9±0.2	0.09	4.7±0.1	4.7±0.3	0.84
Effective stroke volume (ml)	67.8±3.0	69.7±2.2	0.09	67.1±1.5	67.6±4.2	0.84
Pump stroke volume (ml)	110.0±0.2	109.9±0.1	0.73	109.8±0.0	109.8±0.0	0.51
Aortic forward flow time (s)	0.3±0.0	0.3±0.0	0.69	0.3±0.0	0.3±0.0	0.19
Aortic forward volume (ml)	73.3±1.9	73.7±1.9	0.46	73.8±2.0	75.6±1.6	0.19
Aortic valve RMS forward flow rate (ml/s)	306.0±25.2	315.5±14.5	0.33	319.9±6.0	315.6±8.6	0.39
Aortic effective orifice area (cm^2)	1.2±0.5	1.5±0.6	0.13	1.4±0.3	1.2±0.1	0.15
Autograft regurgitant fraction (%)	7.5±3.1	5.5±2.5	0.09	9.0±2.5	10.7±5.3	0.58
Aortic leakage rate (ml/s)	−4.4±3.4	−3.7±2.9	0.67	−5.6±2.8	−7.6±5.7	0.49
Aortic closing volume (ml)	−3.3±1.7	−2.2±0.6	0.08	−3.8±1.6	−4.2±1.2	0.71
TransAortic forward energy loss (mJ)	215.0±165.0	144.6±120.0	0.21	164.0±82.6	212.5±80.6	0.29
TransAortic closing energy loss (mJ)	12.8±7.2	8.1±4.1	0.09	13.1±6.0	13.6±3.7	0.90
TransAortic leakage energy loss (mJ)	31.0±20.0	25.5±18.3	0.62	37.9±17.3	49.3±35.2	0.52
TransAorticl total energy loss (mJ)	258.8±171.8	178.2±124.5	0.14	215.0±98.2	275.4±110.2	0.29

Abbreviations: ACP = anti-commissural plication; RMS = root mean square; SD = standard deviation.

*annotates statistical significance indicated by $p < 0.05$.